Performance evaluation of various distributors and exchange elements configurations in the optical fiber communication system under optimum operating conditions

Article *in* Journal of Optical Communications · March 2023

DOI: 10.1515/joc-2023-0005

Ahmed Nabih Zaki Rashed
faculty of electronic engineering menoufia university

Hasane Ahammad Shaik
K L University

Twana Kak Anwer
Salahaddin University - Erbil

Md. Amzad Hossain
Ruhr-Universität Bochum

Ganesan Shanmugapriya, Suneela Bhoompally, Shaik Hasane Ahammad, Kasi Uday Kiran, Twana Mohammed Kak Anwer, Md. Amzad Hossain*, Ahmed Nabih Zaki Rashed* and Ashraf Ali Nabil

Performance evaluation of various distributors and exchange elements configurations in the optical fiber communication system under optimum operating conditions

https://doi.org/10.1515/joc-2023-0005
Received January 4, 2023; accepted March 4, 2023;
published online March 23, 2023

Abstract: This study reported the performance evaluation of various distributors and exchange elements configurations in the optical fiber communication system. The study of different diaphragm structures mechanics under different pressure levels effects. The stress along the *x* axis of a square diaphragm and the deflection of a square diaphragm under pressure are reported. The radial and tangential stress of a round diaphragm and the deflection of a round diaphragm under pressure are outlined. 3D for the bossed diaphragm deflection against diaphragm position is clarified. The stress distribution across the shorter side of a rectangular diaphragm and 3D for the rectangular diaphragm deflection against diaphragm position under pressure are demonstrated. The radial stress is larger than the tangential stress through the diaphragm radial position from 50 μm to 250 μm for a square diaphragm under pressure. The radial stress is larger than the tangential stress for the bossed diaphragm position varies from 125 μm to 250 μm. All the obtained results are demonstrated through the use of the MEMSolver simulation program software version 3.3.

Keywords: bossed diaphragm; rectangular diaphragm; round diaphragm; square diaphragm; stress.

***Corresponding authors: Md. Amzad Hossain**, Faculty of Electrical Engineering and Information Technology, Institute of Theoretical Electrical Engineering, Ruhr University Bochum, 44801 Bochum, Germany; and Department of Electrical and Electronic Engineering, Jashore University of Science and Technology, Jashore, 7408, Bangladesh, E-mail: mahossain.eee@gmail.com; and **Ahmed Nabih Zaki Rashed**, Electronics and Electrical Communications Engineering Department, Faculty of Electronic Engineering, Menoufia University, Menouf 32951, Egypt; and Department of VLSI Microelectronics, Institute of Electronics and Communication Engineering, Saveetha School of Engineering, SIMATS, Chennai 602105, Tamilnadu, India, E-mail: ahmed_733@yahoo.com. https://orcid.org/0000-0002-5338-1623 (A.N.Z. Rashed)
Ganesan Shanmugapriya, ECE Department, Agnel Institute of Technology and Design, Vasco da Gama, Goa, India, E-mail: spriyagsn@yahoo.com
Suneela Bhoompally, Department of ECE, Malla Reddy Engineering College, Secunderabad, Telagana, 500043, India, E-mail: sunilareddyk@gmail.com
Shaik Hasane Ahammad, Department of ECE, Koneru Lakshmaiah Education Foundation, Vaddeswaram, Andhra Pradesh, 522302, India, E-mail: ahammadklu@gmail.com
Kasi Uday Kiran, Department of ECE, Koneru Lakshmaiah Education Foundation, Guntur, 522502, India, E-mail: uk_ece@kluniversity.in
Twana Mohammed Kak Anwer, Department of Physics, College of Education, Salahaddin University-Erbil, 44002 Erbil, Kurdistan Region, Iraq, E-mail: twana.anwar1@su.edu.krd
Ashraf Ali Nabil, Electronics and Electrical Communications Engineering Department, Faculty of Electronic Engineering, Menoufia University, Menouf 32951, Egypt, E-mail: AshrafAlinabil7675@gmail.com

1 Introduction

As the silicon mechanical structures with the basic beams and the basic diaphragms are the most basic important parts for micro electrical mechanical system (MEMS) devices, the beam mechanics and diaphragm structures will be reviewed in many researches according to the elasticity theory for the homogeneous material [1–12]. There are many types of diaphragms [13–26]. These types can be divided into the square diaphragm, round diaphragm, bossed diaphragm and rectangular diaphragm. Based on the elasticity theory, external forces acting on a solid state body which will cause and produce internal forces between the body portions and cause deformation [27–40]. Depending on its kind and the needs of the network, an optical node is viewed as a multi-purpose component that may carry out a number of functions. In essence, it transmits, receives, and retransmits or reroutes optical signals to its connected neighbours [41–56]. The node must carry out either a routing or switching operation in order to resend or divert an optical signal to the desired networking nodes. It should be noted that several optical multiplexing techniques, such as time division/wavelength division multiplexing, can be utilized. An optical node can also act as a router, sending a certain wavelength of an input signal to a designated output port. Before the signal is sent to the designated output port, it is also possible to alter its wavelength [57–72]. Since it is used to switch the wavelength by converting it to the conforming signal wavelength, the router in this instance will be referred to as a wavelength converting router [73–85]. The physical medium of an optical switch, in contrast to semiconductor switches, remains fixed while performing wavelength operational functions (such as multiplexing, demultiplexing and switching). Integrated optical or optoelectronic devices can be used to create such wavelength changes. The four distinct roles of an optical router are shown in [86–101], where a wavelength demultiplexer is used to split an optical signal with two signal wavelengths (i.e., 1 and 2) present at the input port 1 and route it to ports 2 and 3, respectively [102–125]. Benefits of dense wavelength multiplexing are the transmission with a very high capacity and a very long distance, transparent data transfer. When upgrading systems [126–136], maximum investment protection is provided, high flexibility, efficiency and dependability in networking and support for all-optical switching [137–150].

In this work, the simulative study of a square diaphragm stress and deflection under pressure are demonstrated. As well as a round diaphragm stress and deflection under pressure are also demonstrated. Besides a bossed round diaphragm stress and deflection of are clarified. A rectangular diaphragm stress and deflection are also demonstrated based

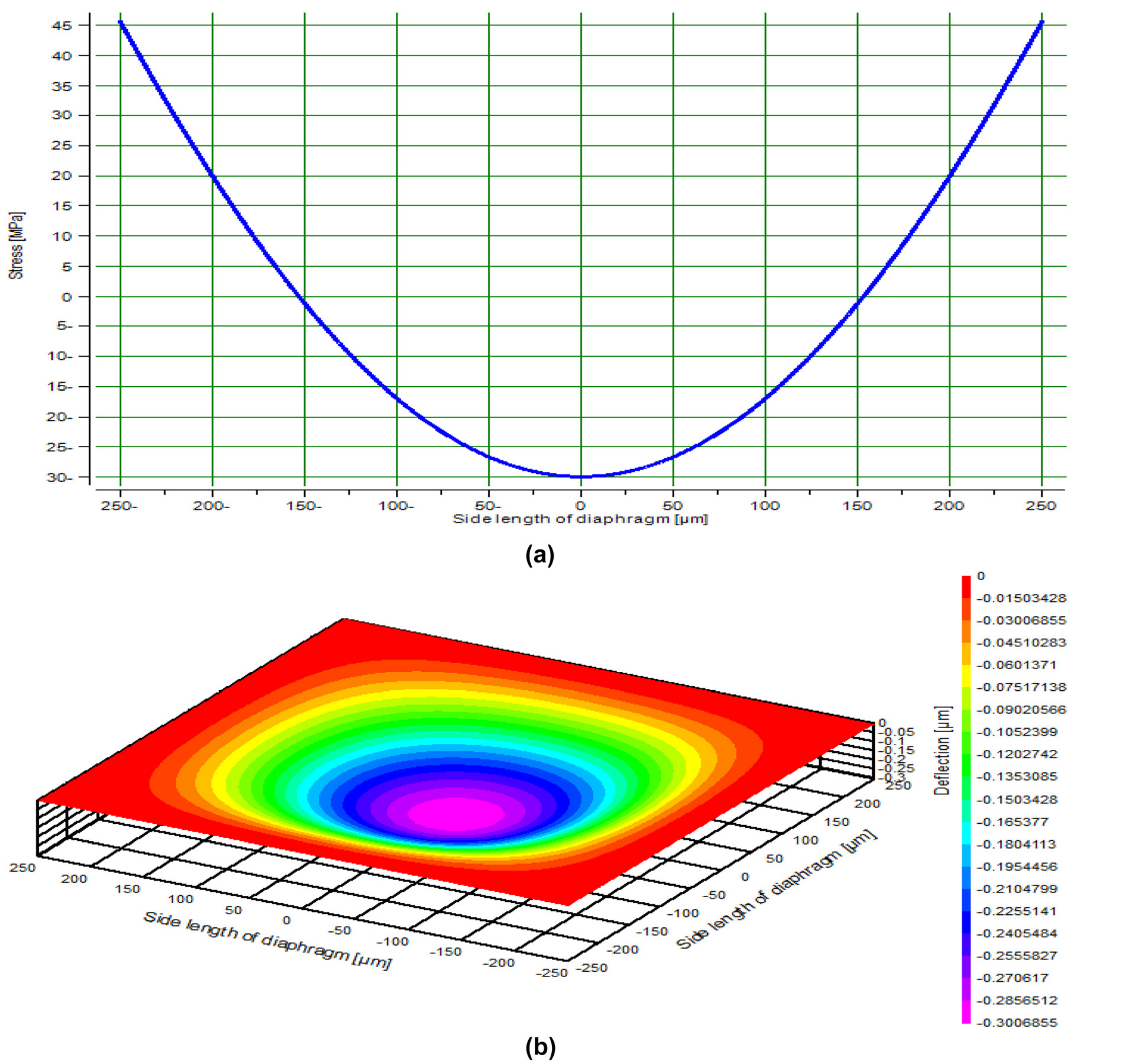

Figure 1: Stress and deflection variations. (a) Stress in relation to diaphragm side length. (b) Deflection of a square diaphragm under pressure.

on MEMSolver simulation program software version 3.3. 3D for the bossed diaphragm deflection against diaphragm position is clarified. The stress distribution across the shorter side of a rectangular diaphragm and 3D for the rectangular diaphragm deflection against diaphragm position under pressure are demonstrated. The radial stress is larger than the tangential stress through the diaphragm radial position from 50 μm to 250 μm for a square diaphragm under pressure. The radial stress is larger than the tangential stress for the bossed diaphragm position varies from 125 μm to 250 μm. All the obtained results are demonstrated through the use of the MEMSolver simulation program software version 3.3.

2 Simulation models description and performance evaluation

Figure 1(a) outlines the stress along the *x* axis of a square diaphragm under pressure. Where the diaphragm side length is 500 μm, diaphragm thickness is 12 μm, applied pressure is 15 psi, Young's modulus (YM) is 180 GPa and Poisson's ratio (PR) is 0.3. The stress increases exponentially with the increase of the diaphragm side length varies from 1 μm to 250 μm. A square diaphragm deflection under pressure effects is shown in Figure 1(b).

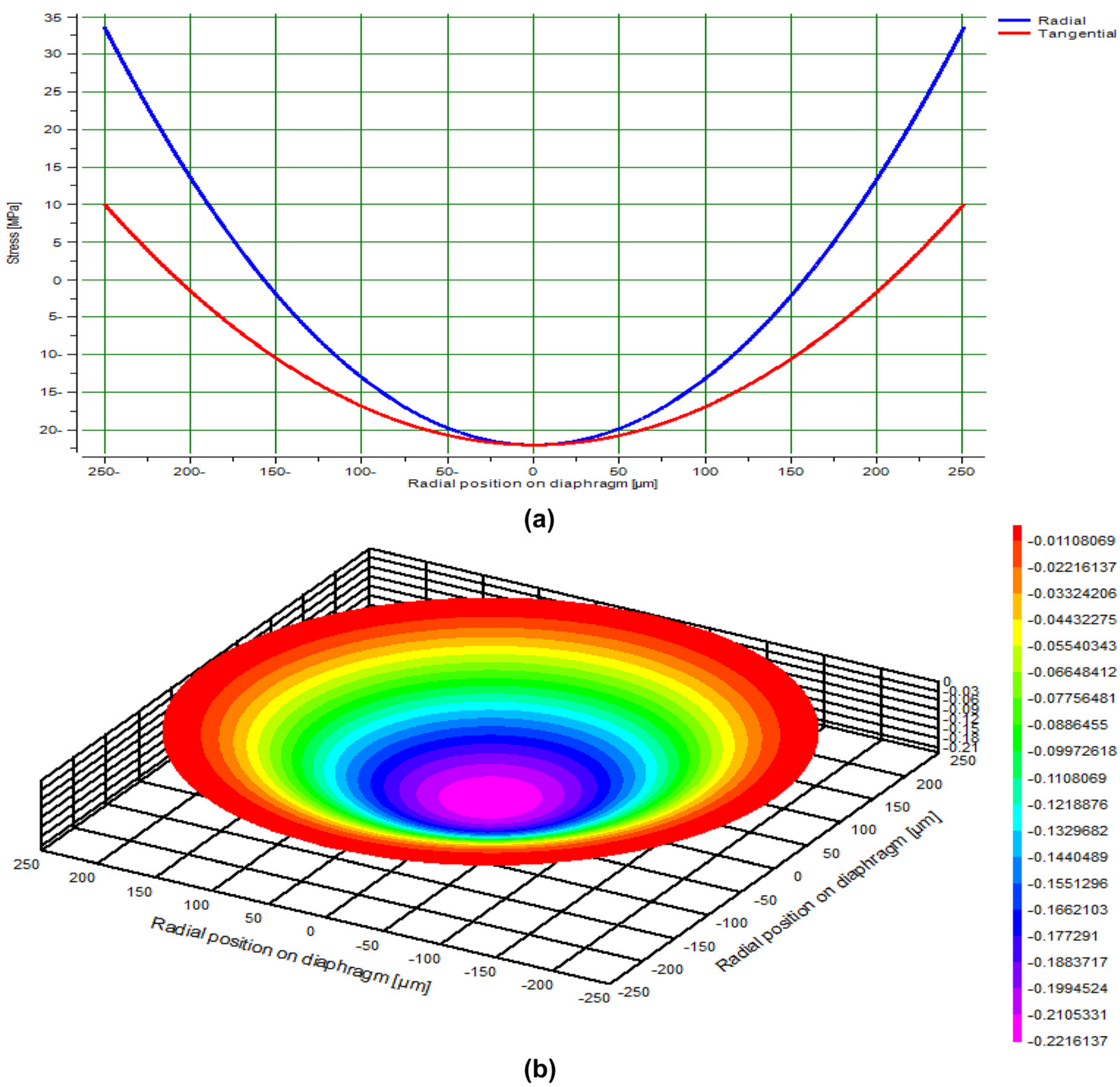

Figure 2: Stress and deflection under pressure effects. (a) Stress versus diaphragm radial position. (b) Deflection of a round diaphragm under pressure.

The square diaphragm stress and deflection under pressure effects are clarified. Where the results assured that the maximum stress is 45.8 MPa, The maximum strain is 254.4 microstrains, and maximum deflection is 0.301 μm.

Figure 2(a) shows the radial and tangential stress of a round diaphragm under pressure. Where the diaphragm diameter is 500 μm, the diaphragm thickness is 12 μm, applied pressure is 15 psi, YM is 180 GPa and PR is 0.3. The stress increases exponentially with the increase of the diaphragm radial position varies from 1 μm to 250 μm. The radial stress is larger than the tangential stress through the diaphragm radial position from 50 μm to 250 μm. The deflection of a round diaphragm under pressure is clarified in Figure 2(b).

The round diaphragm stress and deflection under pressure are reported. The results demonstrated that the maximum stress is 33.7 MPa, the maximum strain is 187.2 microstrains and the maximum deflection is 0.222 μm.

Figure 3(a) demonstrates the deflection of a bossed diaphragm under pressure. Where the diaphragm diameter is 2000 μm, the boss diameter is 700 μm, the diaphragm thickness is 60 μm, applied pressure is 175 psi, PR is 0.3 and

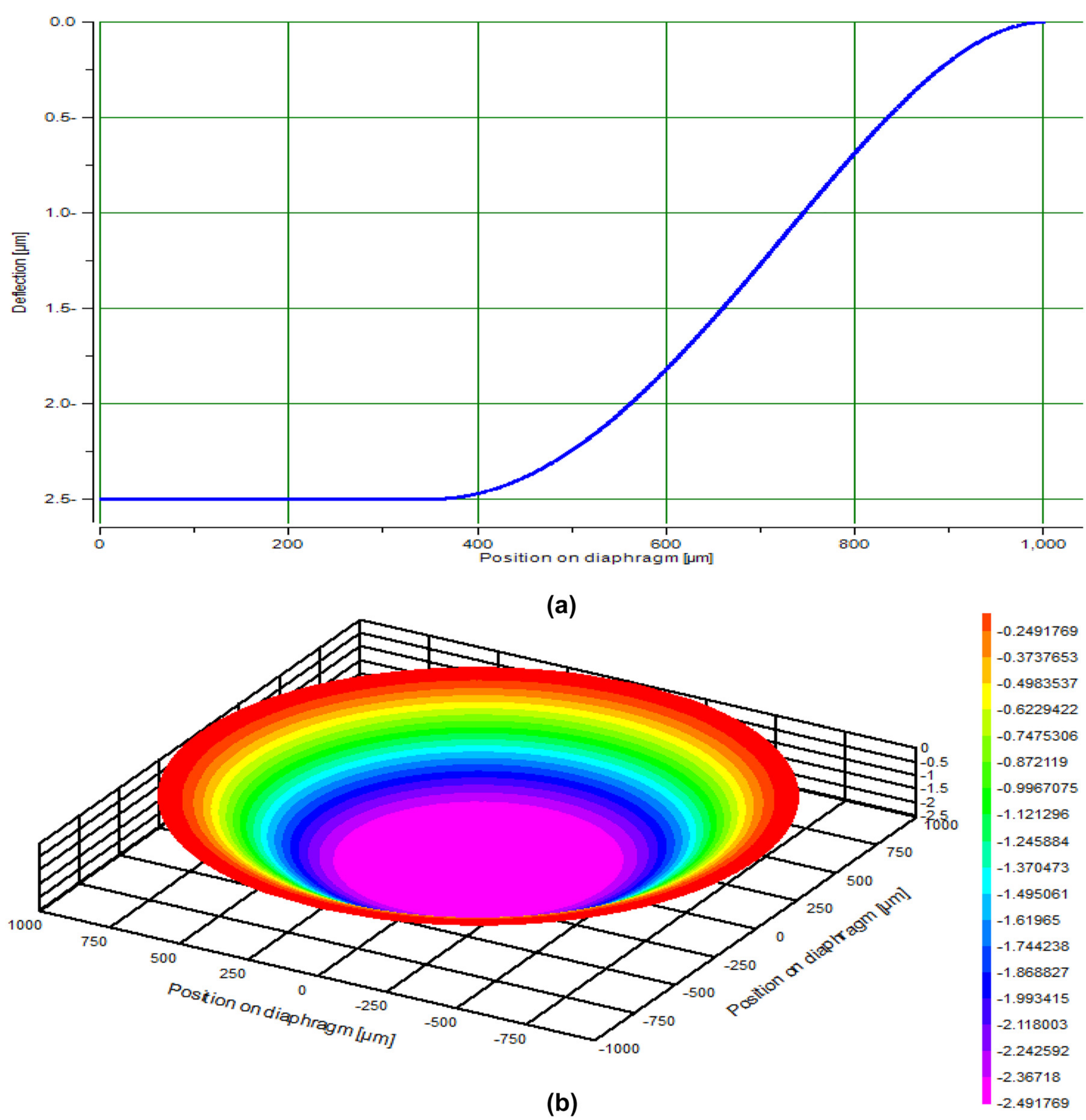

Figure 3: Three dimensional based bossed diaphragm deflection versus diaphragm position. (a) Bossed diaphragm deflection against diaphragm position. (b) 3D for the bossed diaphragm deflection against diaphragm position.

YM is 180 GPa. The bossed diaphragm deflection is almost constant around −2.5 μm for the diaphragm position varies from 1 μm to 400 μm. But the bossed diaphragm deflection is increases exponentially for the diaphragm position varies from 400 μm to 1000 μm. 3D for the bossed diaphragm deflection against diaphragm position is clarified in Figure 3(b).

The maximum bossed diaphragm stress and deflection of under pressure effects are outlined. Where the simulation results assured that the maximum stress is 220.58 MPa, the maximum strain is 1225.44 microstrains and the maximum deflection is 2.492 μm.

Figure 4(a) indicates that the stress distribution across the shorter side of a rectangular diaphragm under pressure. Where the diaphragm length is 700 μm, of diaphragm width is 500 μm, the diaphragm thickness is 9 μm, applied pressure is 15 psi, PR is 0.3 and YM is 180 GPa. Both the radial and tangential stress increases exponentially with the diaphragm position varies from 1 μm to 250 μm. The radial stress is larger than the tangential stress for the diaphragm

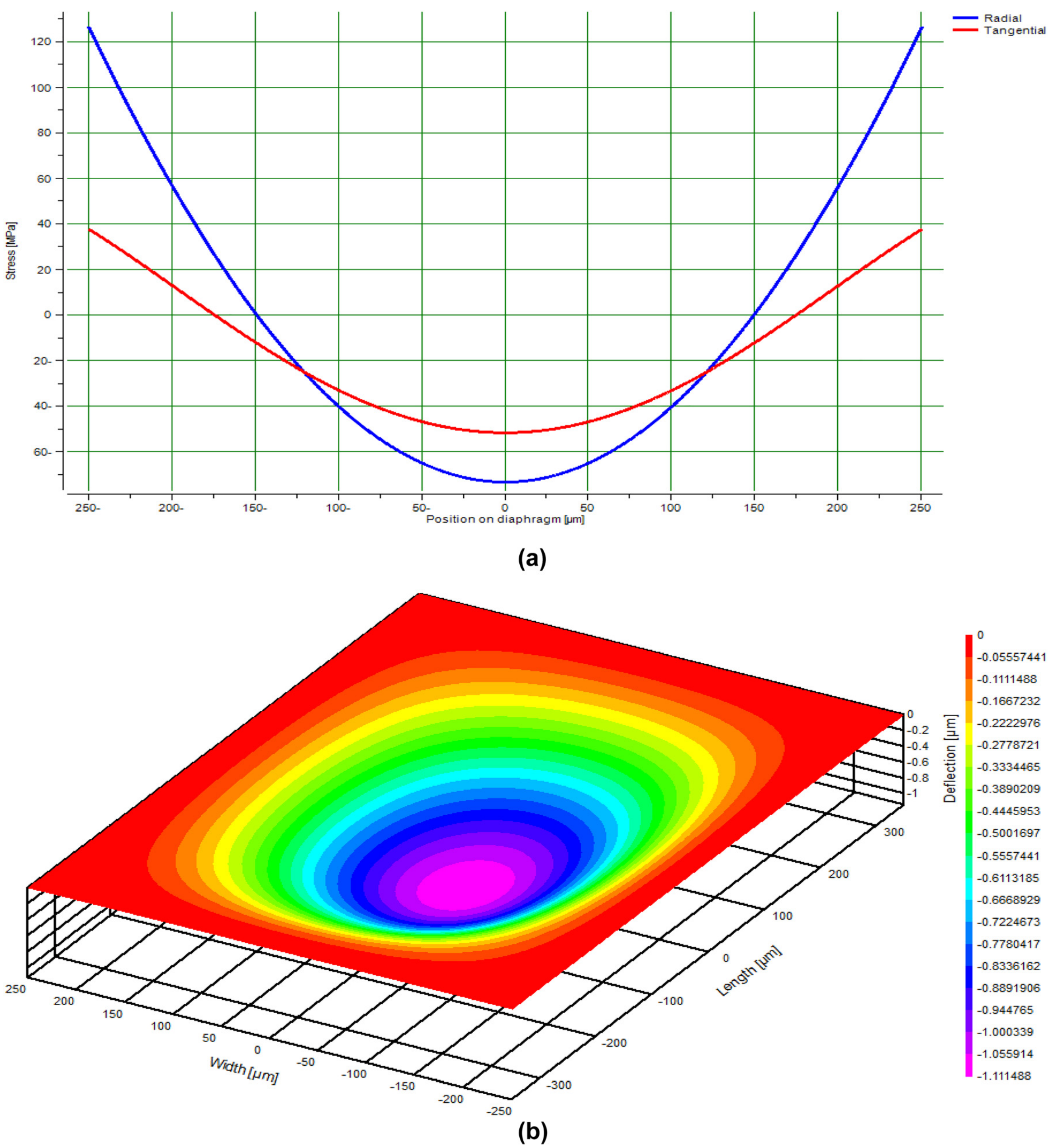

Figure 4: 3D rectangular diaphragm deflection/radial and tangential stress under pressure. (a) Radial and tangential stress versus for rectangular diaphragm position. (b) 3D rectangular diaphragm deflection under pressure.

position varies from 125 µm to 250 µm. 3D for the rectangular diaphragm deflection against diaphragm position is clarified in Figure 4(b).

The maximum rectangular diaphragm stress and deflection under pressure are reported. The results indicated that the maximum stress is 126.6 MPa, The maximum strain is 703.3 microstrains and the maximum deflection is 1.11 µm.

Figure 5 Clarifies the max stress for various diaphragm types under study. The bossed diaphragm is the largest exposed to maximum stress than other proposed types. But the round diaphragm is the largest exposed to minimum stress than other proposed types. Figure 6 Demonstrates the max strain for various diaphragm types under study. The bossed diaphragm is the largest exposed to maximum strain than other proposed types. On the other side the round diaphragm is the largest exposed to minimum strain than other proposed types.

Figure 7 assured the max deflection for various diaphragm types under study. The bossed diaphragm is the largest exposed to maximum deflection than other proposed types. Moreover the round diaphragm is the largest exposed to minimum deflection than other proposed types. Table 1 summarizes the maximum stress, strain, and deflection for various diaphragm at the optimum operating conditions for each case.

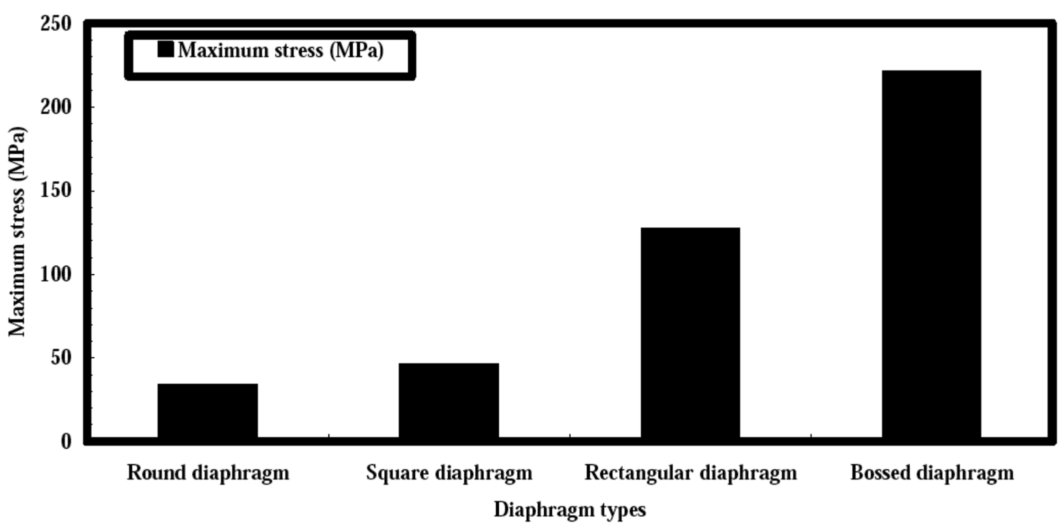

Figure 5: Max. stress with various diaphragm types at the optimum operating parameters.

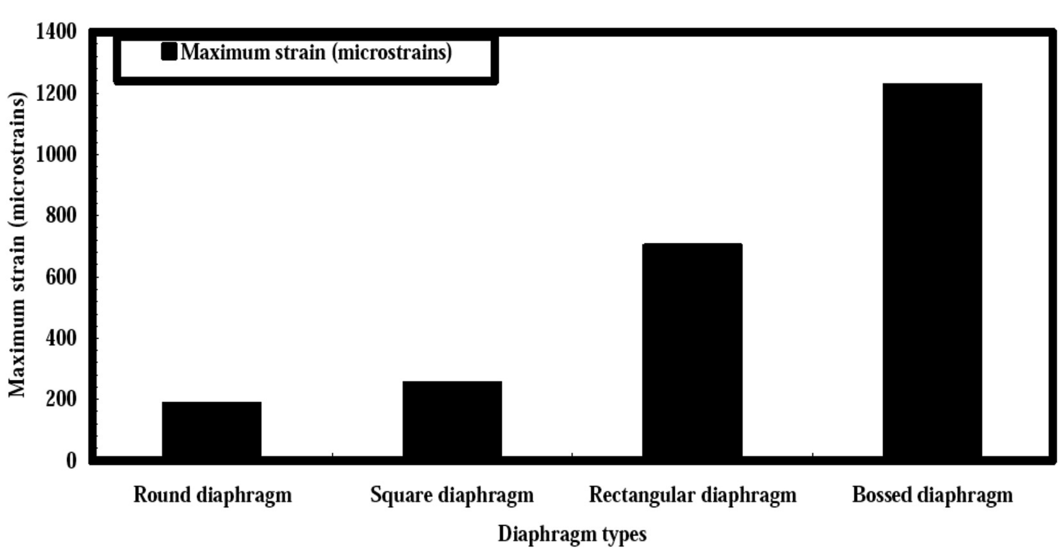

Figure 6: Max. strain with various diaphragm types at the optimum operating parameters.

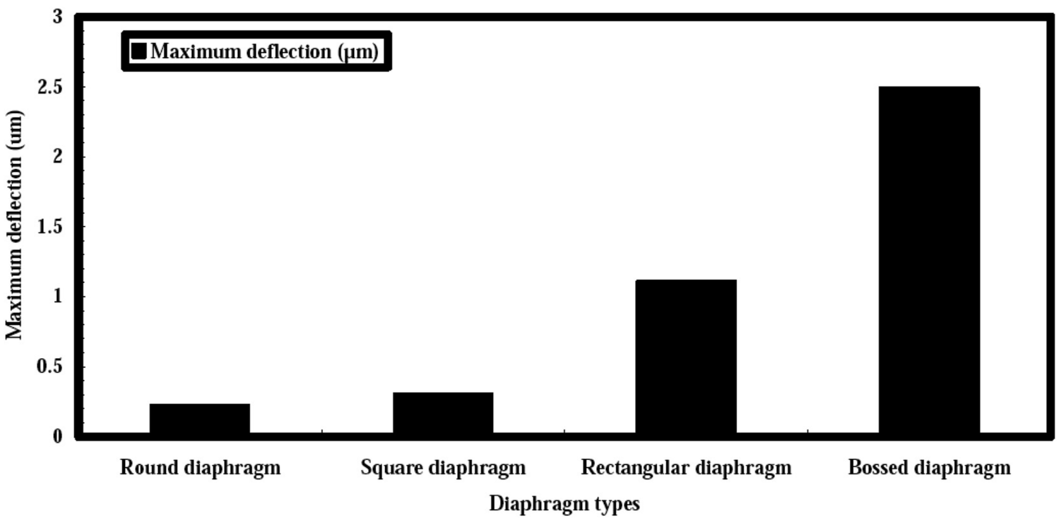

Figure 7: Max. deflection with various diaphragm types at the optimum operating parameters.

Table 1: Maximum stress, strain and deflection for various diaphragm at the optimum operating conditions.

	Various diaphragm types			
	Square diaphragm	**Round diaphragm**	**Bossed diaphragm**	**Rectangular diaphragm**
Maximum stress (MPa)	45.8	33.7	220.58	126.6
Maximum strain (microstrains)	254.4	187.2	1225.44	703.3
Maximum deflection (μm)	0.301	0.222	2.492	1.11

3 Conclusions

We have reviewed the simulative study of different diaphragm structures mechanics under different pressure levels. The study emphasized that the maximum square diaphragm stress and deflection under pressure are clarified the results assured that the maximum stress is 45.8 MPa, The maximum strain is 254.4 microstrains, and maximum deflection is 0.301 μm. The maximum round diaphragm stress and deflection under pressure are reported. The results demonstrated that the maximum stress is 33.7 MPa, the maximum strain is 187.2 microstrains and the maximum deflection is 0.222 μm. The maximum bossed diaphragm stress and deflection under pressure are outlined. Where the simulation results assured that the maximum stress is 220.58 MPa, the maximum strain is 1225.44 microstrains and the maximum deflection is 2.492 μm. The maximum rectangular diaphragm stress and deflection under pressure effects are reported. The results indicated that the maximum stress is 126.6 MPa, The maximum strain is 703.3 microstrains and the maximum deflection is 1.11 μm.

Author contributions: All the authors have accepted responsibility for the entire content of this submitted manuscript and approved submission.
Research funding: None declared.
Conflict of interest statement: The authors declare no conflicts of interest regarding this article.

References

1. Rashed ANZ, Elshamy AM, El-Samie FEA, Faragallah OS, Elshamy EM, El-sayed HS, et al. Optical image cryptosystem using double random phase encoding and Arnold's Cat map. Opt Quant Electron 2016;48: 132–45.
2. Rashed ANZ, Mohamed AENA, Sharshar HA, Tabour MS, El-Sherbeny A. Optical cross connect performance enhancement in optical ring metro network for extended number of users and different bit rates employment. Wireless Pers Commun 2017;94: 927–47.
3. Rashed ANZ, Mohamed AENAEG, Hanafy SAERS, Aly MH. A comparative study of the performance of graded index perfluorinated plastic and alumino silicate optical fibers in internal optical interconnections. Optik 2016;127:9259–63.
4. Rashed ANZ, Mohamed AENA, Mostafa S, El-Samie FEA. Performance evaluation of SAC-OCDMA system in free space optics and optical fiber

system based on different types of codes. Wireless Pers Commun 2017;96:2843–61.
5. Rashed ANZ, Tabbour MSF. Suitable optical fiber communication channel for optical nonlinearity signal processing in high optical data rate systems. Wireless Pers Commun 2017;97:397–416.
6. Rashed ANZ, Tabour MSF, El-Meadawy S. Optimum flat gain with optical amplification technique based on both gain flattening filters and fiber bragg grating methods. J Nanoelectron Optoelectron 2018; 13:665–76.
7. Mohamed SEDN, Mohamed AENA, El-Samie FEA, Rashed ANZ. Performance enhancement of IM/DD optical wireless systems. Photonic Netw Commun 2018;36:114–27.
8. Rashed ANZ, Tabbour MSF. The trade off between different modulation schemes for maximum long reach high data transmission capacity optical orthogonal frequency division multiplexing (OOFDM). Wireless Pers Commun 2018;101:325–37.
9. Rashed ANZ, Kader HMA, Al-Awamry AA, El-Aziz IAA. Transmission performance simulation study evaluation for high speed radio over fiber communication systems. Wireless Pers Commun 2018;103: 1765–79.
10. Rashed ANZ, Tabbour MSF. Best candidate integrated technology for low noise, high speed, and wide bandwidth based transimpedance amplifiers in optical computing systems and optical fiber applications. Int J Commun Syst 2018;31:1–14.
11. Rashed ANZ, Tabbour MSF, El-assar M. 20 Gb/s hybrid CWDM/DWDM for extended reach fiber to the home network applications. Proc Natl Acad Sci India Sect A Phys Sci 2019;89:653–62.
12. Boopathi CS, Kumar KV, Sheebarani S, Selvakumar K, Rashed ANZ, Yupapin P. Design of human blood sensor using symmetric dual core photonic crystal fiber. Results Phys 2018;11:964–5.
13. Vigneswaran D, Rajan MSM, Aly MH, Rashed ANZ. Few-mode ring core fiber characteristics: temperature impact. Photonic Netw Commun 2019;37:131–8.
14. Chakkravarthy SP, Arthi V, Karthikumar S, Rashed ANZ, Yupapin P, Amiri IS. Ultra high transmission capacity based on optical first order soliton propagation systems. Results Phys 2019;12:512–3.
15. Rashed ANZ, Kumar KV, Prithi S, Maheswar R, Tabbour MSF. Transmittivity/reflectivity, bandwidth, and ripple factor level measurement for different refractive index fiber grating shape profiles. J Opt Commun 2019;40:1–15.
16. Rashed ANZ, Kumar KV, Kumar PV, Mohamed AENA, Tabbour MS, El-Assar M. DWDM channel spacing effects on the signal quality for DWDM/CWDM FTTx network. J Opt Commun 2019;40:30–45.
17. Rashed ANZ, Tabbour MSF, Vijayakumari P. Numerical analysis of optical properties using octagonal shaped photonic crystal fiber. J Opt Commun 2019;40:50–65.
18. Rashed ANZ, Kumar SS, Tabbour MSF, Sundararajan TVP, Maheswar R. Different graded refractive index fiber profiles design for the control of losses and dispersion effects. J Opt Commun 2019; 40:75–88.
19. Rashed ANZ. Comparison between NRZ/RZ modulation techniques for upgrading long haul optical wireless communication systems. J Opt Commun 2019;40:100–13.
20. Rashed ANZ, Kumar KV, Tabbour MSF, Sundararajan TVP. Nonlinear characteristics of semiconductor optical amplifiers for optical switching control realization of logic gates. J Opt Commun 2019;40: 122–36.
21. Ahmed K, Paula BK, Vasudevan B, Rashed ANZ, Maheswar R, Amiri IS, et al. Design of D-shaped elliptical core photonic crystal fiber for blood plasma cell sensing application. Results Phys 2019;12:2021–5.
22. Ramana TV, Pandian A, Ellammal C, Jarin T, Rashed ANZ, Sampathkumar A. Numerical analysis of circularly polarized modes in coreless photonic crystal fiber. Results Phys 2019;13:1–13.
23. Rashed ANZ, Mohammed AENA, Zaky WF, Amiri IS, Yupapin P. The switching of optoelectronics to full optical computing operations based on nonlinear metamaterials. Results Phys 2019;13:104–15.
24. Ranathive S, Kumar KV, Rashed ANZ, Tabbour MSF, Sundararajan TVP. Performance signature of optical fiber communications dispersion compensation techniques for the control of dispersion management. J Opt Commun 2019;40:148–57.
25. Amiri IS, Rashed ANZ, Yupapin P. Interaction between optical sources and optical modulators for high-speed optical communication networks. J Opt Commun 2019;40:176–88.
26. Amiri IS, Rashed ANZ, Yupapin P. Effects of order super Gaussian pulses on the performance of high data rate optical fiber channel in the presence of self phase modulation. J Opt Commun 2019;40: 200–12.
27. Amiri IS, Rashed ANZ, Yupapin P. Mathematical model analysis of dispersion and loss in photonic crystal fibers. J Opt Commun 2019;40: 220–30.
28. Amiri IS, Rashed ANZ, Yupapin P. Basic functions of fiber bragg grating effects on the optical fiber systems performance efficiency. J Opt Commun 2019;40:244–54.
29. Amiri IS, Rashed ANZ, Mohammed AENA, Aboelazm MB, Yupapin P. Nonlinear effects with semiconductor optical amplifiers. J Opt Commun 2019;40:266–75.
30. Amiri IS, Rashed ANZ, Yupapin P. High-speed light sources in high-speed optical passive local area communication networks. J Opt Commun 2019;40:288–300.
31. Rashed ANZ, Tabbour MSF, Natarajan K. Performance enhancement of overall LEO/MEO intersatellite optical wireless communication systems. Int J Satell Commun Netw 2020;38:31–40.
32. Amiri IS, Rashed ANZ, Mohammed AEA, El-Din ES, Yupapin P. Spatial continuous wave laser and spatiotemporal VCSEL for high-speed long haul optical wireless communication channels. J Opt Commun 2019; 40:320–30.
33. Amiri IS, Rashed ANZ, Yupapin P. Average power model of optical Raman amplifiers based on frequency spacing and amplifier section stage optimization. J Opt Commun 2019;40:340–55.
34. Amiri IS, Houssien FMAM, Rashed ANZ, Mohammed AENA. Temperature effects on characteristics and performance of near-infrared wide bandwidth for different avalanche photodiodes structures. Results Phys 2019;14:102–10.
35. Amiri IS, Rashed ANZ. Simulative study of simple ring resonator-based brewster plate for power system operation stability. Indones J Electr Eng Comput Sci 2019;16:1070–6.
36. Amiri IS, Rashed ANZ. Different photonic crystal fibers configurations with the key solutions for the optimization of data rates transmission. J Opt Commun 2019;40:377–88.
37. Amiri IS, Rashed ANZ, Ramya KC, Kumar KV, Maheswar R. The physical parameters of EDFA and SOA optical amplifiers and bit sequence variations based optical pulse generators impact on the performance of soliton transmission systems. J Opt Commun 2019;40:400–13.
38. Amiri IS, Houssien FMAM, Rashed ANZ, Mohammed AENA. Optical networks performance optimization based on hybrid configurations of optical fiber amplifiers and optical receivers. J Opt Commun 2019; 40:425–36.
39. Amiri IS, Rashed ANZ, Sarker K, Paul BK, Ahmed K. Chirped large mode area photonic crystal modal fibers and its resonance modes based on finite element technique. J Opt Commun 2019;40:455–65.

40. Amiri IS, Houssien FMAM, Rashed ANZ, Mohammed AENA. Comparative simulation of thermal noise effects for photodetectors on performance of long-haul DWDM optical networks. J Opt Commun 2019;40:477–88.
41. Amiri IS, Rashed ANZ, Mohammed AEA, Aboelazm MB. Single wide band traveling wave semiconductor optical amplifiers for all optical bidirectional wavelength conversion. J Opt Commun 2019;40:503–13.
42. Amiri IS, Rashed ANZ, Mohammed AENA, Zaky WF. Influence of loading, regeneration and recalling elements processes on the system behavior of all optical data bus line system random access memory. J Opt Commun 2019;40:535–44.
43. Malathy S, Kumar KV, Rashed ANZ, Vigneswaran D, Eeldien ES. Upgrading superior operation performance efficiency of submarine transceiver optical communication systems toward multi tera bit per second. Comput Commun J 2019;146:192–200.
44. Amiri IS, Rashed ANZ. Numerical investigation of V shaped three elements resonator for optical closed loop system. Indones J Electr Eng Comput Sci 2019;16:1392–7.
45. Rashed ANZ, Tabbour MSF. The engagement of hybrid dispersion compensation schemes performance signature for ultra wide bandwidth and ultra long haul optical transmission systems. Wireless Pers Commun 2019;109:2399–410.
46. Rashed ANZ, Tabbour MSF, El-Meadawy S, Anwar T, Sarlan A, Yupapin P, et al. The effect of using different materials on erbium-doped fiber amplifiers for indoor applications. Results Phys 2019;15:103–10.
47. Amiri IS, Rashed ANZ. Power enhancement of the U-shape cavity microring resonator through gap and material characterizations. J Opt Commun 2019;40:565–78.
48. Amiri IS, Kuppusamy PG, Rashed ANZ, Jayarajan P, Thiyagupriyadharsan MR, Yupapin P. The engagement of hybrid ultra high space division multiplexing with maximum time division multiplexing techniques for high-speed single-mode fiber cable systems. J Opt Commun 2019;40:588–603.
49. Amiri IS, Rashed ANZ, Jahan S, Paul BK, Ahmed K. Polar polarization mode and average radical flux intensity measurements based on all optical spatial communication systems. J Opt Commun 2019;40:618–28.
50. Sivaranjani S, Sampathkumar A, Rashed ANZ, Sundararajan TVP, Amiri IS. Performance evaluation of bidirectional wavelength division multiple access broadband optical passive elastic networks operation efficiency. J Opt Commun 2019;40:645–60.
51. Amiri IS, Rashed ANZ, Yupapin P. High-Speed transmission circuits signaling in optical communication systems. J Opt Commun 2019;40:675–88.
52. Amiri IS, Rashed ANZ, Jahan S, Paul BK, Ahmed K, Yupapin P. Technical specifications of the submarine fiber optic channel bandwidth/capacity in optical fiber transmission systems. J Opt Commun 2019;40:701–15.
53. Amiri IS, Rashed ANZ. Signal processing criteria based on electro-optic filters for fiber optic access transceiver systems. J Opt Commun 2019;40:733–42.
54. Amiri IS, Rashed ANZ, Yupapin P. Pump laser automatic signal control for erbium-doped fiber amplifier gain, noise figure, and output spectral power. J Opt Commun 2019;40:755–70.
55. Amiri IS, Rashed ANZ, Parvez AHMS, Paul BK, Ahmed K. Performance enhancement of fiber optic and optical wireless communication channels by using forward error correction codes. J Opt Commun 2019;40:786–803.
56. Amiri IS, Rashed ANZ, Yupapin P. Z shaped like resonator with crystal in the presence of flat mirror based standing wave ratio for optical antenna systems. Indones J Electr Eng Comput Sci 2020;17:1405–9.
57. Amiri IS, Rashed ANZ, Yupapin P. Influence of device to device interconnection elements on the system behavior and stability. Indones J Electr Eng Comput Sci 2020;18:843–7.
58. Eid MMA, Amiri IS, Rashed ANZ, Yupapin P. Dental lasers applications in visible wavelength operational band. Indones J Electr Eng Comput Sci 2020;18:890–5.
59. Amiri IS, Rashed ANZ, Yupapin P. Comparative simulation study of multi stage hybrid all optical fiber amplifiers in optical communications. J Opt Commun 2020;41:12–28.
60. Amiri IS, Rashed ANZ, Kader HMA, Al-Awamry AA, El-Aziz IAA, Yupapin P, et al. Optical communication transmission systems improvement based on chromatic and polarization mode dispersion compensation simulation management. Optik 2020;207:163–72.
61. Samanta D, Sivaram M, Rashed ANZ, Boopathi CS, Amiri IS, Yupapin P. Distributed feedback laser (DFB) for signal power amplitude level improvement in long spectral band. J Opt Commun 2020;41:33–43.
62. Amiri IS, Rashed ANZ, Yupapin P. Analytical model analysis of reflection/transmission characteristics of long-period fiber bragg grating (LPFBG) by using coupled mode theory. J Opt Commun 2020;41:55–70.
63. Amiri IS, Rashed ANZ, Rahman Z, Paul BK, Ahmed K. Conventional/phase shift dual drive mach–zehnder modulation measured type based radio over fiber systems. J Opt Commun 2020;41:85–100.
64. Alatwi AM, Rashed ANZ, El-Eraki AM, Amiri IS. Best candidate routing algorithms integrated with minimum processing time and low blocking probability for modern parallel computing systems. Indones J Electr Eng Comput Sci 2020;19:847–54.
65. El-Hageen HM, Alatwi AM, Rashed ANZ. Silicon-Germanium dioxide and aluminum indium gallium arsenide-based acoustic optic modulators. Open Eng J 2020;10:506–11.
66. El-Hageen HM, Alatwi AM, Rashed ANZ. RZ line coding scheme with direct laser modulation for upgrading optical transmission systems. Open Eng J 2020;10:546–51.
67. Alatwi AM, Rashed ANZ, El-Gammal EM. Wavelength division multiplexing techniques based on multi transceiver in low earth orbit intersatellite systems. J Opt Commun 2020;41:113–22.
68. El-Hageen HM, Kuppusamy PG, Alatwi AM, Sivaram M, Yasar ZA, Rashed ANZ. Different modulation schemes for direct and external modulators based on various laser sources. J Opt Commun 2020;41:132–40.
69. El-Hageen HM, Alatwi AM, Rashed ANZ. High-speed signal processing and wide band optical semiconductor amplifier in the optical communication systems. J Opt Commun 2020;41:155–70.
70. El-Hageen HM, Alatwi AM, Rashed ANZ. Laser measured rate equations with various transmission coders for optimum of data transmission error rates. Indones J Electr Eng Comput Sci 2020;20:1406–12.
71. Eid MMA, Habib MA, Anower MS, Rashed ANZ. Highly sensitive nonlinear photonic crystal fiber based sensor for chemical sensing applications. Microsyst Technol 2021;27:1007–14.
72. Eid MMA, Rashed ANZ, Shafkat A, Ahmed K. Fabry perot laser properties with high pump lasers for upgrading fiber optic transceiver systems. J Opt Commun 2020;41:188–200.
73. Eid MMA, Rashed ANZ, Hosen MS, Paul BK, Ahmed K. Spatial optical transceiver system–based key solution for high data rates in measured index multimode optical fibers for indoor applications. J Opt Commun 2020;41:213–22.

74. Eid MMA, Rashed ANZ, El-Meadawy S, Ahmed K. Simulation study of signal gain optimization based on hybrid composition techniques for high speed optically dense multiplexed systems. J Opt Commun 2020; 41:235–50.
75. Alatwi AM, Rashed ANZ. Hybrid CPFSK/OQPSK modulation transmission techniques' performance efficiency with RZ line coding–based fiber systems in passive optical networks. Indones J Electr Eng Comput Sci 2021;21:263–70.
76. Alatwi AM, Rashed ANZ. An analytical method with numerical results to be used in the design of optical slab waveguides for optical communication system applications. Indones J Electr Eng Comput Sci 2021;21:278–86.
77. Alatwi AM, Rashed ANZ. Conventional doped silica/fluoride glass fibers for low loss and minimum dispersion effects. Indones J Electr Eng Comput Sci 2021;21:287–95.
78. El-Hageen HM, Alatwi AM, Rashed ANZ. Spatial optical transmitter based on on/off keying line coding modulation scheme for optimum performance of telecommunication systems. Indones J Electr Eng Comput Sci 2021;21:305–12.
79. Eid MMA, Rashed AANZ, Kurmendra. High speed optical switching gain based EDFA model with 30 Gb/s NRZ modulation code in optical systems. J Opt Commun 2020;41:288–300.
80. Eid MMA, Rashed ANZ, Amiri IS. Fast speed switching response and high modulation signal processing bandwidth through LiNbO3 electro-optic modulators. J Opt Commun 2020;41:312–25.
81. Eid MMA, Houssien FMAM, Rashed ANZ, Mohammed AENA. Performance enhancement of transceiver system based inter satellite optical wireless channel (IS-OWC) for ultra long distances. J Opt Commun 2020;41:345–60.
82. Eid MMA, Rashed ANZ, El-din ES. Simulation performance signature evolution of optical inter satellite links based booster EDFA and receiver preamplifiers. J Opt Commun 2020;41:388–400.
83. Eid MMA, Rashed ANZ, El-gammal EM. Influence of dense wavelength division multiplexing (DWDM) technique on the low earth orbit intersatellite systems performance. J Opt Commun 2020;41:412–26.
84. Eid MMA, Rashed ANZ, Bulbul AAM, Podder E. Mono rectangular core photonic crystal fiber (MRC-PCF) for skin and blood cancer detection. Plasmonics 2021;16:717–27.
85. Eid MMA, Seliem AS, Rashed ANZ, Mohammed AENA, Ali MY, Abaza SS. High speed pulse generators with electro-optic modulators based on different bit sequence for the digital fiber optic communication links. Indones J Electr Eng Comput Sci 2021;21:957–67.
86. Eid MMA, Seliem AS, Rashed ANZ, Mohammed AENA, Ali MY, Abaza SS. The key management of direct/external modulation semiconductor laser response systems for relative intensity noise control. Indones J Electr Eng Comput Sci 2021;21:968–77.
87. Eid MMA, Seliem AS, Rashed ANZ, Mohammed AENA, Ali MY, Abaza SS. Duobinary modulation/predistortion techniques effects on high bit rate radio over fiber systems. Indones J Electr Eng Comput Sci 2021;21: 978–86.
88. Alatwi AM, Rashed ANZ. A pulse amplitude modulation scheme based on in-line semiconductor optical amplifiers (SOAs) for optical soliton systems. Indones J Electr Eng Comput Sci 2021;21:1014–21.
89. Eid MMA, Rashed ANZ, El-Meadawy S, Habib MA. Best selected optical fibers with wavelength multiplexing techniques for minimum bit error rates. J Opt Commun 2020;41:433–43.
90. Alatwi AM, Rashed ANZ, El-Aziz IAA. High speed modulated wavelength division optical fiber transmission systems performance signature. Telkomnika 2021;19:380–9.
91. Eid MMA, Rashed ANZ, El-gammal EM, Delwar TS, Ryu JY. The influence of electrical filters with sequence generators on optical ISL performance evolution with suitable data rates. J Opt Commun 2020; 41:455–70.
92. Alatwi AM, Rashed ANZ, Parvez AHMS, Paul BK, Ahmed K. Beam divergence and operating wavelength bands effects on free space optics communication channels in local access networks. J Opt Commun 2020;41:488–500.
93. Shafkat A, Rashed ANZ, El-Hageen HM, Alatwi AM. The effects of adding different adhesive layers with a microstructure fiber sensor based on surface plasmon resonance: a numerical study. Plasmonics 2021;16:819–32.
94. Eid MMA, Rashed ANZ. Fiber optic propagation problems and signal bandwidth measurements under high temperature and high dopant germanium ratios. J Opt Commun 2020;41:512–22.
95. Eid MMA, Rashed ANZ. Simulative and analytical methods of bidirectional EDFA amplifiers in optical communication links in the optimum case. J Opt Commun 2020;41:533–50.
96. Eid MMA, Shehata E, Rashed ANZ. Cascaded stages of parametric optical fiber amplifiers with Raman fiber amplifiers for upgrading of telecommunication networks through optical wireless communication channel. J Opt Commun 2020;41:566–76.
97. Eid MMA, Mohammed AENA, Rashed ANZ. Simulative study on the cascaded stages of traveling wave semiconductor optical amplifiers based multiplexing schemes for fiber optic systems improvement. J Opt Commun 2020;41:588–600.
98. Parvin T, Ahmed K, Alatwi AM, Rashed ANZ. Differential optical absorption spectroscopy based refractive index sensor for cancer cell detection. Opt Rev 2021;28:134–43.
99. Eid MMA, Said SM, Rashed ANZ. Gain/noise figure spectra of average power model Raman optical amplifiers in coarse wavelength multiplexed systems. J Opt Commun 2020;41:613–22.
100. Eid MMA, Rashed ANZ, Ahammad MS, Paul BK, Ahmed K. The effects of Tx./Rx. pointing errors on the performance efficiency of local area optical wireless communication networks. J Opt Commun 2020;41: 633–43.
101. Eid MMA, El-Hamid HSA, Rashed ANZ. High-speed fiber system capacity with bidirectional Er-Yb CDFs based on differential phase shift keying (DPSK) modulation technique. J Opt Commun 2020;41:654–66.
102. Eid MMA, Ibrahim A, Rashed ANZ. In line and post erbium-doped fiber amplifiers with ideal dispersion compensation fiber Bragg grating for upgrading optical access networks. J Opt Commun 2020;41:688–700.
103. Eid MMA, Ahmed H, Rashed ANZ. Chirped Gaussian pulse propagation with various data rates transmission in the presence of group velocity dispersion (GVD). J Opt Commun 2020;42:13–22.
104. Habib A, Rashed ANZ, El-Hageen HM, Alatwi AM. Extremely sensitive photonic crystal fiber–based cancer cell detector in the terahertz regime. Plasmonics 2021;16:1297–306.
105. Shafkat A, Rashed ANZ, El-Hageen HM, Alatwi AM. Design and analysis of a single elliptical channel photonic crystal fiber sensor for potential malaria detection. J Sol Gel Sci Technol 2021;98:202–11.
106. Eid MMA, Rashed ANZ. Fixed scattering section length with variable scattering section dispersion based optical fibers for polarization mode dispersion penalties. Indones J Electr Eng Comput Sci 2021;21: 1540–7.
107. Eid MMA, Seliem AS, Rashed ANZ, Mohammed AENA, Ali MY, Abaza SS. High sensitivity sapphire FBG temperature sensors for the signal processing of data communications technology. Indones J Electr Eng Comput Sci 2021;21:1567–74.

108. Eid MMA, Seliem AS, Rashed ANZ, Mohammed AENA, Ali MY, Abaza SS. High modulated soliton power propagation interaction with optical fiber and optical wireless communication channels. Indones J Electr Eng Comput Sci 2021;21:1575–83.
109. Eid MMA, Rashed ANZ, Delwar TS, Siddique A, Ryu JY. Linear/cubic measured pulse numerically with electrical jitter amplitude variations for the impact on fiber communication systems. J Opt Commun 2021; 42:33–43.
110. Eid MMA, El-Meadawy S, Mohammed AENA, Rashed ANZ. Wavelength division multiplexing developed with optimum length-based EDFA in the presence of dispersion-compensated fiber system. J Opt Commun 2021;42:55–70.
111. Eid MMA, Sorathiya V, Lavadiya S, Habib MA, Helmy A, Rashed ANZ. Dispersion compensation FBG with optical quadrature phase shift keying (OQPSK) modulation scheme for high system capacity. J Opt Commun 2021;42:86–100.
112. Eid MMA, Sorathiya V, Lavadiya S, Shehata E, Rashed ANZ. Free space and wired optics communication systems performance improvement for short-range applications with the signal power optimization. J Opt Commun 2021;42:114–22.
113. Eid MMA, Rashed ANZ. Numerical simulation of long-period grating sensors (LPGS) transmission spectrum behavior under strain and temperature effects. Sens Rev 2021;41:192–9.
114. Eid MMA, Rashed ANZ. Basic FBG apodization functions effects on the filtered optical acoustic signal. Indones J Electr Eng Comput Sci 2021; 22:287–96.
115. Eid MMA, El-Meadawy S, Mohammed AENA, Rashed ANZ. High data rates in optic fiber systems based on the gain optimization techniques. J Opt Commun 2021;42:130–44.
116. Ahmed K, AlZain MA, Abdullah H, Luo Y, Vigneswaran D, Faragallah OS, et al. Highly sensitive twin resonance coupling refractive index sensor based on gold- and MgF2-coated nano metal films. Biosensors 2021; 11:104–13.
117. Delwar TS, Siddique A, Biswal MR, Rashed ANZ, Jee AJ, Ryu Y. Novel multi-user MC-CSK modulation technique in visible light communication. Opt Quant Electron 2021;53:196–206.
118. Eid MMA, Habib MA, Anower MS, Rashed ANZ. Hollow core photonic crystal fiber (PCF)–Based optical sensor for blood component detection in terahertz spectrum. Braz J Phys 2021;51:1017–25.
119. Eid MMA, Sorathiya V, Lavadiya S, El-Hamid HSA, Rashed ANZ. Wide band fiber systems and long transmission applications based on optimum optical fiber amplifiers lengths. J Opt Commun 2021;42: 155–70.
120. Eid MMA, Sorathiya V, Lavadiya S, Shehata E, Rashed ANZ. Optical switches based semiconductor optical amplifiers (SOAs) for performance characteristics enhancement by using various electrical pulse generators. J Opt Commun 2021;42:183–95.
121. Eid MMA, Rashed ANZ, Sorathiya V, Lavadiya S, Habib MA, Amiri IS. GaAs electro-optic absorption modulators performance evaluation, under high-temperature variations. J Opt Commun 2021;42:200–13.
122. Abdullaha H, Ahmed K, Alama MS, Rashed ANZ, Mitua SA, Al-Zahranid FA, et al. High sensitivity refractive index sensor based on triple layer MgF2-gold-MgF2 coated nano metal films photonic crystal fiber. Optik 2021;241:166–76.
123. Eid MMA, Sorathiya V, Lavadiya S, El-Aziz IAA, Rashed ANZ. Free space optics communication channel with amplitude/frequency shift keying modulation technique based raised cosine line coding. J Opt Commun 2021;42:225–36.
124. Eid MMA, Rashed ANZ, Rajagopal M, Parimanam J, Abhay V. Integrated role between VCSEL diodes and Gaussian pulse generators with ideal EDFA for self phase modulation instability management. J Opt Commun 2021;42:255–70.
125. Eid MMA, Sorathiya V, Lavadiya S, Helmy A, Rashed ANZ. Technical specifications and spectral performance characteristics of dispersion flattened fiber (DFF) in optical fiber systems. J Opt Commun 2021;42: 280–95.
126. Eid MMA, Rashed ANZ. Hybrid NRZ/RZ line coding scheme based hybrid FSO/FO dual channel communication systems. Indones J Electr Eng Comput Sci 2021;22:866–73.
127. Bulbul AAM, Rashed ANZ, El-Hageen HM, Alatwi AM. Design and numerical analysis of an extremely sensitive PCF-based sensor for detecting kerosene adulteration in petrol and diesel. Alex Eng J 2021; 60:5419–30.
128. Eid MMA, Sorathiya V, Lavadiya S, El-Aziz IAA, Asaduzzaman S, Rehana H, et al. ROF systems performance efficiency based on continuous phase frequency shift keying phase modulation scheme. J Opt Commun 2021;42:305–13.
129. Habib MA, Anower MS, Ahmed AG, Faragallah OS, Eid MMA, Rashed ANZ. Efficient way for detection of alcohols using hollow core photonic crystal fiber sensor. Opt Rev 2021;28:383–92.
130. Eid MMA, Sorathiya V, Lavadiya S, Parmar J, Patel SK, Ali SA, et al. CWDM communication system based inline erbium-doped fiber amplifiers with the linear geometrical polarization model. J Opt Commun 2021;42:320–33.
131. Sorathiya V, Lavadiya S, Ahmed AG, Faragallah OS, El-sayed HS, Eid MMA, et al. A comparative study of broadband solar absorbers with different gold metasurfaces and MgF2 on tungsten substrates. J Comput Electron 2021;20:1840–50.
132. Lavadiya SP, Sorathiya V, Kanzariya S, Chavda B, Faragallah OS, Eid MMA, et al. Design and verification of novel low profile miniaturized pattern and frequency tunable microstrip patch antenna using two PIN diodes. Braz J Phys 2021;51:1303–13.
133. Eid MMA, Urooj S, Alwadai NM, Rashed ANZ. AlGaInP optical source integrated with fiber links and silicon avalanche photo detectors in fiber optic systems. Indones J Electr Eng Comput Sci 2021;23:847–54.
134. Urooj S, Alwadai NM, Ibrahim A, Rashed ANZ. Simulative study of raised cosine impulse function with Hamming grating profile based Chirp Bragg grating fiber. J Opt Commun 2021;42:350–65.
135. Jibon RH, Bulbul AAM, Nahid AA, Faragallah OS, Baz M, Eid MMA, et al. Design and numerical analysis of a photonic crystal fiber (PCF)-based flattened dispersion THz waveguide. Opt Rev 2021;28:564–72.
136. Eid MMA, Mohammed AENA, Rashed ANZ. Different soliton pulse order effects on the fiber communication systems performance evaluation. Indones J Electr Eng Comput Sci 2021;23:1485–92.
137. Urooj S, Alwadai NM, Sorathiya V, Lavadiya S, Parmar J, Patel SK, et al. Differential coding scheme based FSO channel for optical coherent DP-16 QAM transceiver systems. J Opt Commun 2021;42:377–90.
138. Rashed ANZ, Zaky WF, Eid MMA, Faragallah OS. Dynamic response based on non-linear material for electrical and optical analogy of full optical oscillator. Opt Quant Electron 2021;53:234–50.
139. Rashed ANZ, Zaky WF, El-Hageen HM, Alatwi AM. Technical specifications for an all-optical switch for information storage and processing systems. Eur Phys J Plus 2021;136:1100–12.
140. Sorathiya V, Lavadiya S, Parmar B, Das S, Krishna M, Faragallah OS, et al. Numerical investigation of the tunable polarizer using gold array and graphene metamaterial structure for an infrared frequency range. Appl Phys B 2022;128:555–70.

141. Delwar TS, Siddique A, Biswal MR, Behera P, Rashed ANZ, Choi Y, et al. A novel dual mode configurable and tunable high-gain, high-efficient CMOS power amplifier for 5G applications. Integrat VLSI J 2022;83: 77–87.
142. Eid MMA, Arunachalam R, Sorathiya V, Lavadiya S, Patel SK, Parmar J, et al. QAM receiver based on light amplifiers measured with effective role of optical coherent duobinary transmitter. J Opt Commun 2022; 43:20–33.
143. Sorathiya V, Lavadiya S, Ahmed AG, Faragallah OS, El-Sayed HS, Parmar B, et al. Hilbert resonator based multiband tunable graphene metasurface polarizer for lower THz frequency. J Comput Electron 2022;21:280–8.
144. Mohammad A, Alzaidi MS, Eid MMA, Sorathiya V, Lavadiya S, Patel SK, et al. First order surface grating fiber coupler under the period chirp and apodization functions variations effects. Indones J Electr Eng Comput Sci 2022;25:1020–9.
145. Mohammad A, Alzaidi MS, Eid MMA, Sorathiya V, Lavadiya S, Patel SK, et al. Free space optical communication system for indoor applications based on printed circuit board design. Indones J Electr Eng Comput Sci 2022;25:1030–7.
146. Sorathiya V, Lavadiya S, Parmar BS, Baxi S, Dhankot T, Faragallah OS, et al. Tunable squared patch based graphene metasurface infrared polarizer. Appl Phys B 2022;128:247–60.
147. Lavadiya S, Sorathiya V, Faragallah OS, El-Sayed HS, Eid MMA, Rashed ANZ. Infrared graphene assisted multi-band tunable absorber. Opt Quant Electron 2022;54:145–65.
148. Jibon RH, Ahmed M, Abd-Elnaby M, Rashed ANZ, Eid MMA. Design mechanism and performance evaluation of photonic crystal fiber (PCF) based sensor in the THz regime for sensing noxious chemical substrates of poultry feed. Appl Phys A 2022;128:1656–66.
149. Sorathiya V, Lavadiya S, Thomas L, Abd-Elnaby M, Rashed ANZ, Eid MMA. Graphene based tunable short band absorber for infrared wavelength. Appl Phys B 2022;128:101–16.
150. Dutta N, Patel SK, Faragallah OS, Baz M, Rashed ANZ. Caching scheme for information-centric networks with balanced content distribution. Int J Commun Syst 2022;35:16–29.